Structure of *Trypanosoma cruzi* glycosomal glyceraldehyde-3-phosphate dehydrogenase complexed with chalepin, a natural product inhibitor, at 1.95 Å resolution

F. Pavão[a,b], M.S. Castilho[b], M.T. Pupo[c], R.L.A. Dias[d], A.G. Correa[d], J.B. Fernandes[d], M.F.G.F. da Silva[d], J. Mafezoli[d], P.C. Vieira[d], G. Oliva[b,*]

[a] *Instituto de Química de São Carlos, USP, São Carlos, SP, Brazil*
[b] *Instituto de Física de São Carlos, USP, P.O. Box 369, 13560-970 São Carlos, SP, Brazil*
[c] *Faculdade de Ciências Farmacêuticas de Ribeirão Preto, USP, Ribeirão Preto, SP, Brazil*
[d] *Departamento de Química, UFSCar, P.O. Box 676, 13560-000 São Carlos, SP, Brazil*

Received 21 January 2002; revised 3 April 2002; accepted 5 April 2002

First published online 26 April 2002

Edited by Hans Eklund

Abstract The structure of the glycosomal glyceraldehyde-3-phosphate dehydrogenase (gGAPDH) from *Trypanosoma cruzi* complexed with chalepin, a natural product from *Pilocarpus spicatus*, has been determined by X-ray crystallography to 1.95 Å resolution. The structure is in the apo form without cofactors in the subunits of the tetrameric gGAPDH in the asymmetric unit. Unequivocal density corresponding to the inhibitor was clearly identified in one monomer. The final refined model of the complex shows extensive conformational changes when compared with the native structure. The mode of binding of chalepin to gGAPDH and its implications for inhibitor design are discussed.

Key words: Glyceraldehyde-3-phosphate dehydrogenase; Natural product; Chalepin; X-ray crystallography; *Trypanosoma cruzi*

1. Introduction

Some protozoan parasites of the family Trypanosomatidae cause a wide variety of severe diseases such as the American trypanosomiasis known as Chagas' disease. Some 100 million persons – a quarter of all the inhabitants of Latin America – are at risk of contracting the disease and an estimated 16–18 million people are infected [1]. Chagas' disease is caused by infection with the parasite *Trypanosoma cruzi*. It is transmitted by the blood-sucking *Triatomine* insects, through blood transfusions or congenitally from infected mothers. No effective treatment is available for the disease [2].

The modern approach of target-directed drug development involves the identification of suitable enzymes taking part in essential metabolic pathways of pathogens. Several peculiarities in the biology of trypanosomatids have been suggested to be exploitable for drug design purposes [3]. Trypanosomatids are highly dependent on glycolysis for ATP production [4,5] and the in silico modeling of the pathway has indicated the reaction catalyzed by glycosomal glyceraldehyde-3-phosphate dehydrogenase (gGAPDH) as one of the preferred steps for inhibition [6,7]. The enzyme catalyzes the oxidative phosphorylation of D-glyceraldehyde-3-phosphate into 1,3-diphosphoglycerate in the presence of NAD^+ and inorganic phosphate. Structural studies of the enzymes from *Trypanosoma brucei* [8] and *Leishmania mexicana* [9] have shown differences in the NAD^+ cofactor binding pocket when compared with the human homologue, which lead to the design and synthesis of several inhibitors focusing on this site [10–13]. Aiming at the design of novel classes of anti-chagasic drugs, the structure of the *T. cruzi* gGAPDH was determined and described elsewhere [14]. Computational search procedures [15] and extensive screening of plant extracts through the enzymatic inhibitory assays have been performed in the search for promising lead compounds [15–17]. Several coumarins were found as the most promising class of substances from natural sources with significant gGAPDH inhibitory activity. Amongst them is chalepin (Fig. 1), a coumarin extracted from *Pilocarpus spicatus*, which has an IC_{50} (inhibitor concentration required for 50% inhibition of enzymatic activity) of 64 μM [17].

In order to elucidate the mechanism of inhibition and the specific mode of binding of this inhibitor, and to elicit further improvement of this molecule through structure-based drug design, we present here the crystallographic structure of gGAPDH from *T. cruzi* complexed with chalepin.

2. Materials and methods

2.1. Preparation and purification of T. cruzi gGAPDH

Recombinant *T. cruzi* gGAPDH was prepared and purified according to a previously reported procedure [14].

2.2. Extraction, isolation and identification of chalepin

The air-dried powdered stem of *P. spicatus* (Rutaceae) was exhaustively extracted with organic solvents (hexane, CH_2Cl_2 and MeOH) through percolation processing at room temperature. Crude extracts were obtained after evaporation of the solvents under reduced pressure at 40°C. The hexane extract (PSSH, 6.0 g) was fractionated through liquid–liquid partition with hexane–methanol–water (10:9:1) followed by ethyl acetate–methanol–water (1:1:1) and butanol–methanol–water (1:1:2). The ethyl acetate fraction (PSSH/A, 1.3 g) was chromatographed on a silica gel column using a step gradient of hexane and ethyl acetate. Successive flash chromatography of the fraction eluted with 20–30% hexane/ethyl acetate allowed the isolation of the 6-(1,1-dimethylallyl)-2-(1-hydroxy-1-methylethyl)-2,3-dihydro-7*H*-furo[3,2-*g*]chromen-7-one, a coumarin known as chalepin (45 mg). The structure of chalepin was deduced on the basis of its spectral

*Corresponding author. Fax: (55)-16-2739881.
E-mail address: oliva@if.sc.usp.br (G. Oliva).

0014-5793/02/$22.00
PII: S0014-5793(02)02700-X

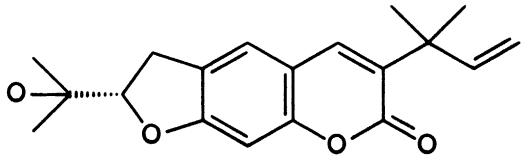

Fig. 1. Chalepin.

data (^{1}H and ^{13}C nuclear magnetic resonance and mass spectrometry), which were confirmed by comparative analysis with the literature values [18].

2.3. Enzymatic inhibition studies

The enzymatic activities of *T. cruzi* gGAPDH and its human homologue and the inhibitory activity of chalepin against these enzymes have been determined according to a previously reported procedure [17], using the forward reaction.

The IC_{50} was determined empirically. A wide range of concentrations (10–100 μg/ml) of inhibitor were tested at substrate and cofactor saturating conditions. The percentage of remaining activity was calculated by comparison with an inhibitor-free control experiment.

The chalepin showed no inhibition of human GAPDH activity while it showed an IC_{50} of 64 μM against *T. cruzi* gGAPDH, as mentioned above.

2.4. Co-crystallization assays

Co-crystallization assays were carried out using a protein solution at 8 mg/ml in 0.1 M TEA pH 7.6, 1 mM NAD^+, 1 mM DTT, 1 mM PMSF, 1 mM EDTA, 1 μM leupeptin and 1 μM pepstatin pre-incubated with 5 mM of inhibitor and 10% (v/v) of acetonitrile. Crystals of the complex gGAPDH–chalepin were grown at 22°C by vapor diffusion, against a reservoir solution of 0.1 M sodium cacodylate pH 6.9–7.1, with 0.1 M calcium acetate, 16–18% of polyethylene glycol 8000, in a microgravity environment during flight STS-91 of the NASA US Space Shuttle program. Mechanical damage upon landing and transport of crystals resulted in few crystals being available for data collection.

2.5. Data collection and processing

Crystals of the gGAPDH–chalepin complex were flash-cooled to 100 K in an Oxford Cryostream Cooler. The cryoprotectant solution used consists of 20% polyethylene glycol 400 added to the above described reservoir solution. The X-ray source was a Rigaku RU-200 rotating anode generator operating at 50 kV/100 mA. Diffraction intensities were collected with an R-AXIS II image plate, using the rotation method [19]. Data processing was carried out with programs DENZO and SCALEPACK [20]. Final electron density maps for each collected data set revealed that only in one crystal the inhibitor could be unambiguously modelled. Data collection and processing statistics for this data set are summarized in Table 1. The experiment had to be interrupted after 120 frames due to loss of cryogenic protection. All available and well measured data were included in the refinement, on the basis that the program used does take care adequately of low intensity data, through proper weighting of weak observations. The criterion used to decide on the cut-off of the data was to limit the resolution when $I/\sigma(I)$ was above 1.0 and the R_{merge} was below 50%.

Crystals belong to the space group $P2_1$ with unit cell parameters $a = 82.08$ Å, $b = 84.97$ Å, $c = 105.24$ Å and $\beta = 96.32°$. The analysis of crystal contents indicates one tetramer per asymmetric unit and a V_m value of 2.34 Å^3/Da.

Table 1
Statistics of X-ray data collection and processing

Rotation angle	1.0°
Total number of frames	120
Total collected reflections	195 798
Number of unique reflections	81 630
Resolution limit	1.95 Å
Completeness	77.9% [38.1%]
R_{merge}	10.7% [48.3%]
$I/\sigma(I)$	6.78 [1.1]
Redundancy	2.4 [1.6]

The values in brackets correspond to the last resolution shell (2.02–1.95 Å)

Table 2
Final refinement statistics

Resolution range	15–1.95 Å
Amino acid residues per monomer	359
Water molecules	937
Inhibitor molecule in the a.u.	1
R_{factor}	0.201
$R_{free,3\%}$	0.280
RMS bond deviations	0.015 Å
RMS angle deviations	3.1°

2.6. Structure determination and refinement

The structure of the chalepin complex was determined by molecular replacement, using the program AMoRe [21]. The native gGAPDH structure without ligands or water molecules was used as the search model. Using diffraction data in the resolution range 15.0–4.0 Å, the top solution showed correlation coefficient of 61.3% and R_{factor} of 35.7%. The rotated and translated model was refined using REFMAC [22], the electron density maps and omit maps were calculated using FFT [23] and OMIT [24], respectively, all from the CCP4 suite of programs [25]. Manual rebuilding of the macromolecular model and graphics visualization were performed using the O software [26]. The crystallographic R_{factor} and $R_{free,3\%}$ values, as well as the stereochemistry quality of the model (program PROCHECK [27]), were constantly monitored during the course of the refinement.

The first cycle was a rigid body refinement, with only the quaternary structure of the model tetramer being allowed to change while the four individual subunits were held as rigid bodies. This refinement produced a R_{factor} of 0.398 and R_{free} of 0.405. $2F_{obs}-F_{calc}$ and $F_{obs}-F_{calc}$ electron density maps calculated from this model showed no density in the cofactor binding sites which could be interpretable as NAD^+. This fact clearly indicated the interference of the inhibitor over the enzyme. Thus, the following cycles of restrained crystallographic refinement were carried out without non-crystallographic symmetry to search for any bound inhibitor to the tetramer. A difference ($F_{obs}-F_{calc}$) electron density map calculated after 10 cycles of automated restrained refinement showed density in the active site of the C subunit resembling the inhibitor. At this point, the R_{factor} was 0.252 and R_{free} was 0.322. After several iterative cycles of restrained refinement of the atomic coordinates followed by visual manipulation, water molecules were automatically built into the model using the program ARP [28]. After inclusion of 630 water molecules the R_{factor} dropped to 0.209 and R_{free} to 0.282. At this stage a molecule of chalepin was manually built into the electron density observed at the C subunit active site. The final cycles of refinement included the addition of another 307 waters, as well as the refinement of partial occupancies for the inhibitor and the two alternative conformations for the –SH group of active site Cys^{166} of subunit C. The results are summarized in Table 2.

2.7. Protein data bank accession number

The atomic coordinates of the *T. cruzi* gGAPDH–chalepin co-crystal structure and the structure factor amplitudes have been deposited with the Protein Data Bank under ID code 1K3T.

3. Results and discussion

3.1. Quality of the structure

The final $2F_{obs}-F_{calc}$ electron density maps calculated for the gGAPDH–chalepin complex show good quality (Fig. 2). The stereochemistry of the structure is, in general, quite satisfactory, with more than 99% of the residues showing torsion angles in the favorable regions of the Ramachandran diagram [29]. Only Ala^{73} from the C subunit and Val^{255} from all subunits are in unfavorable regions. Ala^{73} is located in a flexible loop at the N-terminal, which shows poor electron density,

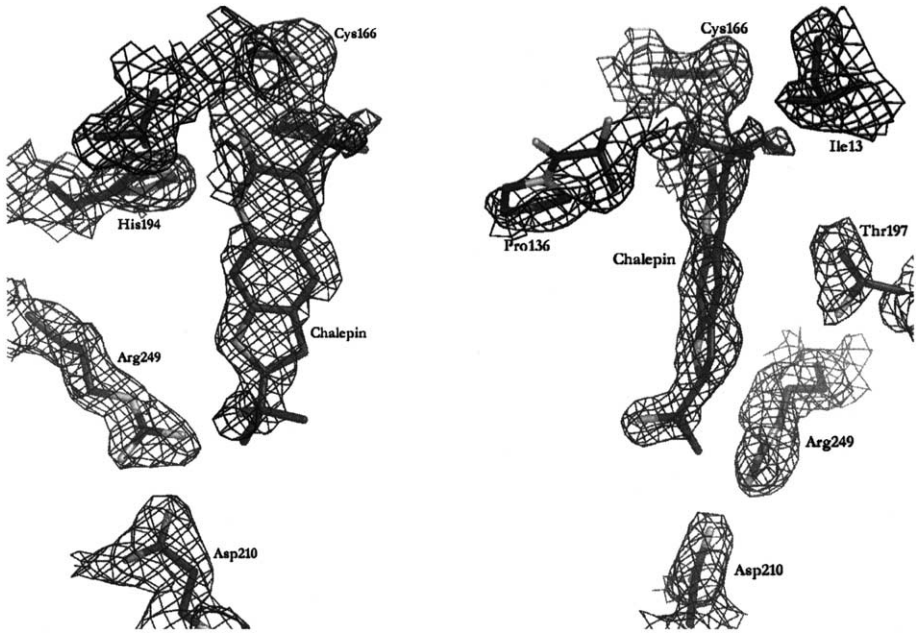

Fig. 2. Electron density omit maps ($2F_{obs}-F_{calc}$) of the GAPDH–chalepin complex, close to the active site, contoured at 1.3σ level. Unambiguous density for the natural product inhibitor is seen. Figure produced with the program PyMOL Molecular Graphics System - DeLano Scientific.

causing difficulties to appropriately model its torsion angles. Val^{255} is located in a loop between two consecutive β-strands and its uncommon conformation is conserved in all other GAPDH structures available [8,9,14,30,31] and is important to maintain the correct positioning of the active residue Cys^{166} with respect to the nicotinamide ring of the NAD^+ cofactor during catalysis.

The average temperature factor values for the main chain and all atoms of the 359 residues from each subunit are, respectively, 24.3 $Å^2$ and 25.2 $Å^2$, to the A subunit, 29.9 $Å^2$ and 30.7 $Å^2$, to the B subunit, 42.8 $Å^2$ and 43.3 $Å^2$, to the C subunit and 25.0 $Å^2$ and 26.1 $Å^2$, to the D subunit. The average temperature factor value for all atoms of chalepin is 70.8 $Å^2$. The higher values of the average temperature factor observed for the C subunit reflect the static disorder resulting from the partial occupancy of the inhibitor (85%) at its active site. Analysis of the crystal packing shows that the NAD^+ binding domain of subunit C has no lattice contacts, compatible with alternative domain rotations.

3.2. *Structural differences between gGAPDH complexed with chalepin (apo form, without NAD^+) and the native holo form*

The four individual subunits of the gGAPDH tetramer are related to each other by a 222 non-crystallographic symmetry. Each subunit is composed of two domains: the NAD^+ binding domain, comprising residues 1–150 at the N-terminal and residues 331–359 at the C-terminal; and the catalytic domain,

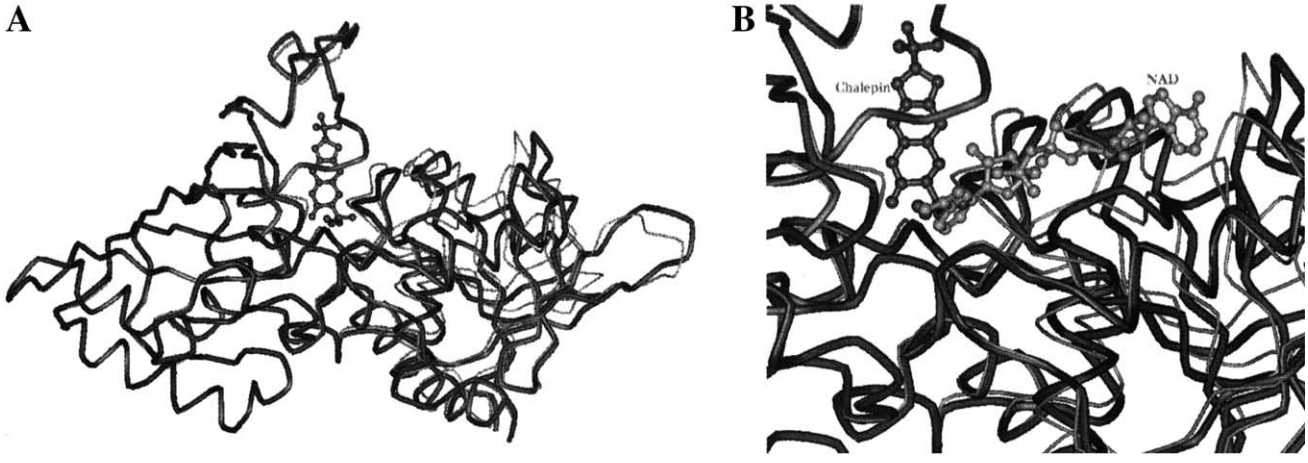

Fig. 3. A: Superposition of the native *T. cruzi* gGAPDH structure (thin ribbon) and chalepin complex (thick ribbon) with the inhibitor displayed. The catalytic domain (left) was included in the superposition protocol. B: Close-up of the active site with ligands. The NAD^+ is bound to the native structure whereas the chalepin is bound in the complex structure. The clash observed in the region of the nicotinamide moiety of NAD^+ explains why the binding of the inhibitor implies in the displacement of the cofactor, therefore stabilizing the apo structure of the enzyme. Figure produced with the program Web Lab Viewer (Molecular Simulations Inc.).

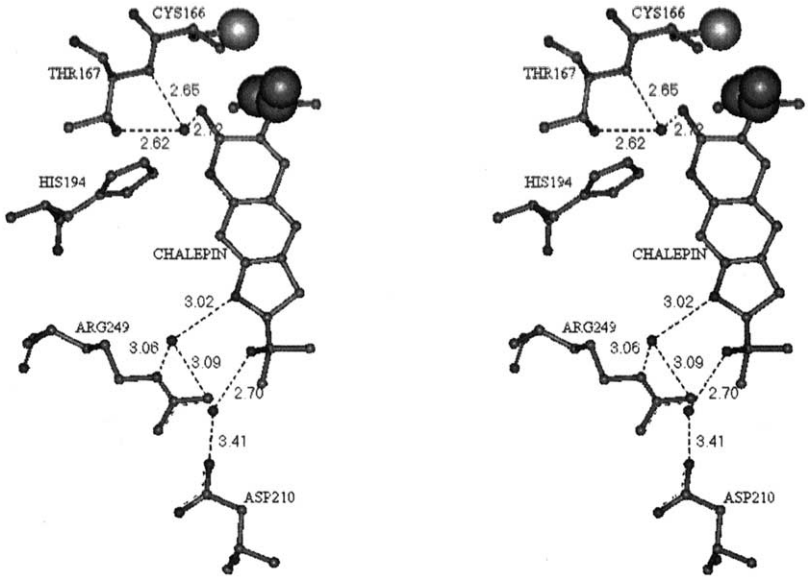

Fig. 4. Stereoview of the overall mode of binding of chalepin to gGAPDH active site. Figure produced with the program Web Lab Viewer [Molecular Simulations Inc.].

comprising residues 151–330. The tetramer of GAPDH is formed exclusively through contacts between all four catalytic domains, constituting a rigid core of the tetrameric particle that remains virtually unchanged in both native and complex structures. The displacement of the NAD^+ cofactor by the binding of the inhibitor induces the holo to apo transition, represented predominantly by an approximate rigid-body rotation of 4° of the NAD binding domain of each subunit relative to the structurally conserved catalytic domain (Fig. 3). Other internal modifications of the NAD^+ binding domain are also present. This feature has previously been observed in the apo and holo forms of GAPDH and liver alcohol dehydrogenase enzymes from other sources [32–34]. The authors suggested that the overall effect of this conformational change is to expose the cofactor and active site to solvent in the apo form and provide additional shield of the cofactor and active site from solvent in the holo form. Indeed, the tetrameric holoenzyme shows a solvent-accessible surface area of 46 051 $Å^2$ while the apo-enzyme has a surface area of 49 152 $Å^2$. The solvent-accessible surface buried upon ligand binding at subunit C is 205 $Å^2$.

3.3. gGAPDH–chalepin interaction architecture

Of the possible 525 $Å^2$ of solvent-accessible surface area in the free inhibitor, 209 $Å^2$ are exposed to solvent in the complex and 316 $Å^2$ are buried upon binding. The analysis of the complex shows three important interacting groups from chalepin (Fig. 4). The carbonyl oxygen from lactonic group interacts with residue Thr^{167} by hydrogen bonds mediated by a water molecule W^{739}. The 1,1-dimethylallyl group interacts by hydrophobic contacts with catalytic residue Cys^{166}, which has to undergo a conformational change through a rotation of χ_1,

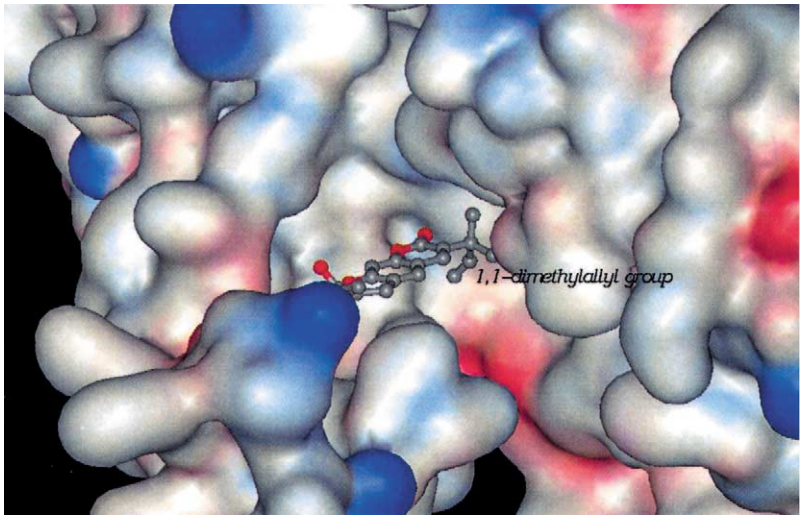

Fig. 5. View of the chalepin binding site. The neighboring regions of the 1,1-dimethylallyl group, which remain unoccupied after binding of the inhibitor, show charged residues which can be exploited in the design of new chalepin derivatives. Molecular surface of the gGAPDH generated with the program Web Lab Viewer [Molecular Simulations Inc.].

in order to accommodate the positioning of the inhibitor at the active site. Indeed, the final electron density maps show the two alternative conformations of Cys^{166}, one of them apparently connecting to the inhibitor. This is an artifact, since the side chain of this residue is at the native conformation only when the inhibitor is absent. Therefore, the evident two conformations of the Cys^{166} side chain guarantee that the inhibitor has to have partial occupancy. Finally, the oxygen atom from the benzo-dihydrofuran group interacts with residue Arg^{249} through a hydrogen bond mediated by water molecule W^{813}. The 1-hydroxy-1-methylethyl group interacts weakly with the residue Asp^{210} by hydrogen bond mediated by a water molecule W^{812}.

3.4. Implications for drug design approach

Based on this analysis, modifications in the chalepin inhibitor can be suggested by molecular modeling studies. At the 1,1-dimethylallyl binding site it is evident (Fig. 5) that there are neighboring regions with charged residues, which remain unoccupied after binding of the inhibitor. It is therefore possible to design the replacement of the 1,1-dimethylallyl group by substituents containing heteroatoms like nitrogen, oxygen or halogens. These modifications could enable the formation of new dipole–dipole interactions resulting in energetic gain notably greater than the hydrophobic interactions observed in the crystal structure. Besides, Souza et al. [14] suggest that the substitution of Asp^{210} (*T. cruzi*) by Leu^{194} (human) brings a new target for selective inhibition. The chalepin 1-hydroxy-1-methylethyl group does not interact efficiently with the protein. The introduction of a linker arm of one or two carbon atoms may cause a closer contact between the chalepin hydroxyl and the Asp^{210} delta2 oxygen atom, producing more effective polar interactions and increasing specificity for the parasitic enzyme. New proposed coumarin derivatives are being synthesized and tested against *T. cruzi* gGAPDH to evaluate these possibilities.

Acknowledgements: The authors are grateful to FAPESP (CEPID program), WHO (TDR Grant 940854), the Howard Hughes Medical Institute, PADCT-SBIO and CNPq for financial support.

References

[1] World Health Organisation Statistical Information System Web Site, at http://www.who.int/ctd/chagas.
[2] Urbina, J.A. (1999) Mem. Inst. Oswaldo Cruz 94. (Suppl. I), 349–355.
[3] Barrett, M.P., Mottram, J.C. and Coombs, G.H. (1999) Trends Microbiol. 7, 82–88.
[4] Opperdoes, F.R. (1987) Annu. Rev. Microbiol. 41, 127–151.
[5] Opperdoes, F.R. and Michels, P.A.M. (2001) Int. J. Parasitol. 31, 482–490.
[6] Bakker, B.M., Michels, P.A.M., Opperdoes, F.R. and Westerhoff, H.V. (1999) J. Biol. Chem. 274, 14551–14559.
[7] Bakker, B.M., Westerhoff, H.V., Opperdoes, F.R. and Michels, P.A.M. (2000) Mol. Biochem. Parasitol. 106, 1–10.
[8] Velieux, F.M.D., Hajdu, J., Verlinde, C.L.M.J., Groendijk, H., Read, R.J., Greenhough, T.J., Campbell, J.W., Kalk, K.H., Littlechild, J.A., Watson, H.C. and Hol, W.G.J. (1993) Proc. Natl. Acad. Sci. USA 90, 2355–2359.
[9] Kim, H., Feil, I.K., Verlinde, C.L.M.J., Petra, P.H. and Hol, W.G.J. (1995) Biochemistry 34, 14975–14986.
[10] Callens, M. and Hannaert, V. (1995) Ann. Trop. Med. Parasitol. 89 (Suppl. 1), 23–30.
[11] Aronov, A.M., Verlinde, C.L.M.J., Hol, W.G.J. and Gelb, M.H. (1998) J. Med. Chem. 41, 4790–4799.
[12] Aronov, A.M., Suresh, S., Buckner, F.S., Voorhis, W.C.V., Verlinde, C.L.M.J., Opperdoes, F.R., Hol, W.G.J. and Gelb, M.H. (1999) Proc. Natl. Acad. Sci. USA 96, 4273–4278.
[13] Suresh, S., Bressi, J.C., Kennedy, K.J., Verlinde, C.L.M.J., Gelb, M.H. and Hol, W.G.J. (2001) J. Mol. Biol. 309, 423–435.
[14] Souza, D.H.F., Garrat, R.C., Araújo, A.P.U., Guimarães, B.G., Jesus, W.D.P., Michels, P.A.M., Hannaert, V. and Oliva, G. (1998) FEBS Lett. 424, 131–135.
[15] Monteiro, M.R., Vieira, P.C., Fernandes, J.B., Silva, M.F.G.F., Pupo, M.T., Pavão, F., Oliva, G. and Albuquerque, S. (1997) Mem. Inst. Oswaldo Cruz 92 (Suppl. I), 325.
[16] Tomazela, D.M., Pupo, M.T., Passador, E.A., Silva, M.F., Vieira, P.C., Fernandes, J.B., Fo, E.R., Oliva, G. and Pirani, J.R. (2000) Phytochemistry 55, 643–651.
[17] Vieira, P.C., Mafezoli, J., Pupo, M.T., Fernande, J.B., Silva, M.F.G.F., Albuquerque, S., Oliva, G. and Pavão, F. (2001) Pure Appl. Chem. 73, 617–622.
[18] Oliveira, F.M., Sant'ana,, A.E.G., Conserva, L.M., Maia, J.G.S. and Guilhon, G.M.P. (1996) Phytochemistry 41, 647–649.
[19] Arndt, U.W. and Wonacott, A.J. (1977) The Rotation Method in Crystallography. North-Holland, Amsterdam.
[20] Otwinowski, Z. and Minor, W. (1997) Methods Enzymol. 276, 307–326.
[21] Navaza, J. (1994) Acta Crystallogr. A50, 157–163.
[22] Murshudov, G.N., Vagin, A.A. and Dodson, E.J. (1997) Acta Crystallogr. D53, 240–255.
[23] Ten Eyck, L.F. (1973) Acta Crystallogr. A29, 183–191.
[24] Bhat, T.N. (1988) J. Appl. Crystallogr. 21, 279–281.
[25] Bailey, S. (1994) Acta Crystallogr. D50, 760–763.
[26] Jones, T.A., Zou, J.Y., Cowan, S.W. and Kjeldgaard, M. (1991) Acta Crystallogr. A47, 110–119.
[27] Laskowski, R.A., Macarthur, M.W., Moss, D.S. and Thornton, J.M. (1993) J. Appl. Crystallogr. 26, 283–291.
[28] Lamzin, V.S. and Wilson, K.S. (1993) Acta Crystallogr. D49, 129–147.
[29] Ramachandran, G.N., Ramakrishnan, C. and Sasisekharan, V. (1963) J. Mol. Biol. 7, 95–99.
[30] Watson, H.C., Mercer, W.D. and Duee, E. (1972) Nature New Biol. 240, 130–139.
[31] Skarżyński, T., Moody, P.C.E. and Wonacott, A.J. (1987) J. Mol. Biol. 193, 171–187.
[32] Skarżyński, T. and Wonacott, A.J. (1988) J. Mol. Biol. 203, 1097–1118.
[33] Murthy, M.R.N., Garavito, R.M., Johnson, J.E. and Rossmann, M.G. (1980) J. Mol. Biol. 138, 859–872.
[34] Eklund, H., Samama, J.P., Wallen, L., Branden, C.I., Akeson, A. and Jones, T.A. (1981) J. Mol. Biol. 146, 561–587.